

PLANAR NEAR-FIELD MEASUREMENT RESULTS UP TO 94 GHz USING PROBE POSITION CORRECTION

Jeff Guerrieri, Katie MacReynolds, Mike Francis, Ron Wittmann, and Doug Tamura
National Institute of Standards and Technology, 818.02
Boulder, CO 80305

Abstract

This paper presents results of planar near-field measurements at 16, 35 and 94 GHz using probe position correction algorithms. The algorithms correct for position errors of the probe near the scan plane. The probe's actual position is measured using a laser tracker integrated into the planar-near-field scanning system at NIST. The laser tracker simultaneously obtains probe-position information at each point where amplitude and phase data are acquired during planar near-field antenna measurements.

Keywords: laser tracker, planar near-field, position-error correction, probe-position correction.

1.0 Introduction

This paper is a continuation of work presented at the 2004 AMTA Symposium [1]. The previous paper discussed the use of a laser tracking device to provide probe-position information in x, y, and z coordinate which can be used with recently developed algorithms [2,3] to compensate for displacement errors in the actual measurement positions. Planar near-field (PNF) measurements were performed at 16 and 35 GHz using the laser tracker. Corrected probe position results are shown for these measurements.

This paper presents the results of the 16 and 35 GHz measurements along with the results of measurements performed at 94 GHz, using the position-correction algorithms.

When the probe can be positioned within $\lambda/50$ at each data point in the measurement grid, the position uncertainty is negligible for side-lobe levels down to -40 dB below the peak. Reasonable position accuracy for PNF scanners is ± 0.03 cm in x, y, and z, which allows for accurate antenna

measurements up to about 20 GHz. For less precise (more economical) scanners, this upper frequency limit may be even lower. Table 1 lists values of wavelength (λ), and the $\lambda/50$ criteria for the frequency range 1-500 GHz.

Table 1. $\lambda/50$ guidelines for PNF measurements.

Freq. (GHz)	λ (cm)	$\lambda/50$ (cm)
1.0	30.00	0.6000
16.0	1.875	0.0375
35.0	0.857	0.0171
50.0	0.600	0.0120
94.0	0.319	0.0064
110.0	0.273	0.0055
325.0	0.092	0.0018
500.0	0.060	0.0012

To accurately perform PNF measurements above a scanner's upper frequency limit, based on mechanical probe positioning accuracies, NIST has developed probe position correction (PPC) algorithms [2,3]. To correct for probe position errors the true coordinates of the probe at each measurement must be determined within the $\lambda/50$ accuracies listed in Table 1. The measurement uncertainty of the laser tracker setup used at NIST is ± 0.0001 cm.

2.0 Procedure

Figure 1 shows the tracking system as it was positioned and used on the planar scanner in the NIST laboratory. The laser head was mounted on a stable tripod and placed so its view was unobstructed through the measurement cycle. A target mirror was mounted to the probe assembly and moved across the scan plane with the probe. Since the target mirror is metallic, it was positioned on the side of the probe assembly behind RF absorber to eliminate reflections that might interfere with the electromagnetic measurements.

* U.S. government work, not U.S. copyright protected.

To define the position and orientation of the scan plane, the laser tracker was used to measure the position of the probe at three points: 1) x_{\min}, y_{\min} ; 2) x_{\max}, y_{\min} ; 3) x_{\max}, y_{\max} .

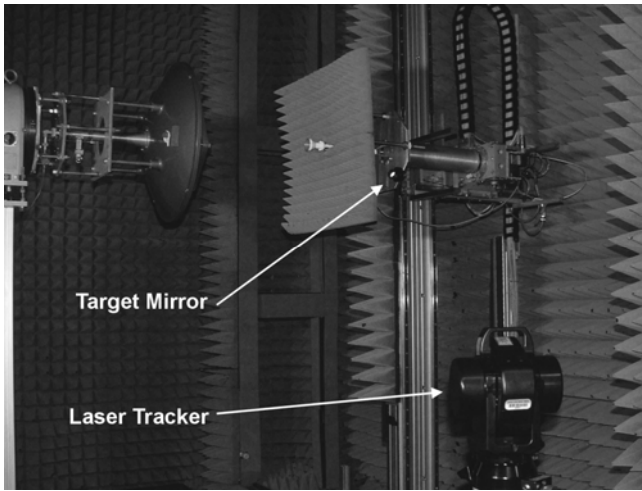


Figure 1. Laser tracker setup for PNF measurements.

3.0 Measurements and Results

A Cassegrain reflector dish and probe in the WR-62 band were used for the 16 GHz measurements. The z-position errors in the plane used in the 16 GHz measurements were as large as ± 0.02 cm (see Figure 2). According to Table 1 this is about 7% more than the recommended limit.

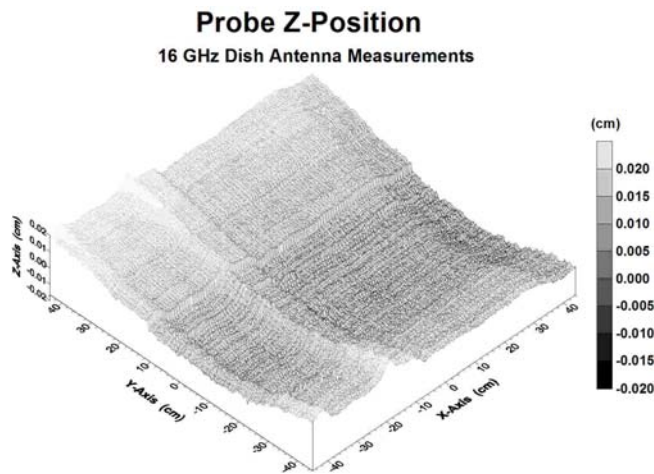


Figure 2. Probe z-position errors for 16 GHz PNF measurements.

If we look at the near-field amplitude before and after probe-position correction (PPC) in Figures 3 and 4, we see little effect.

Furthermore, if we look at the coupled far field amplitude, (this is the coupling product because the effects of the probe are not removed) of the measurement before and after probe position correction, in Figures 5 and 6, we see a negligible effect.

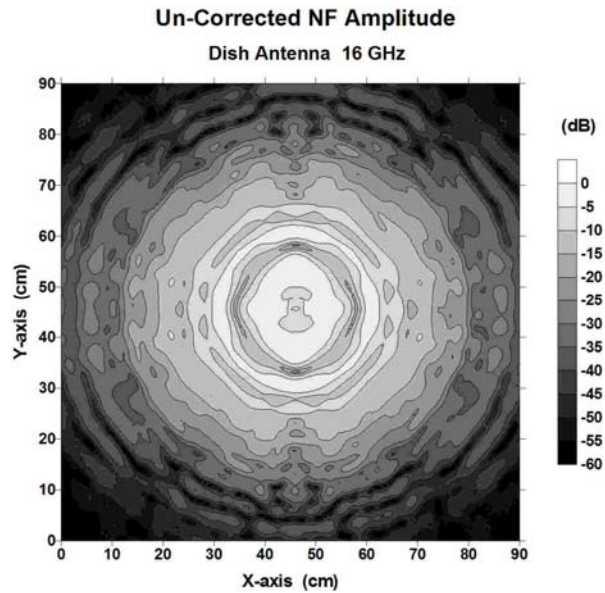


Figure 3. Near-field amplitude for 16 GHz measurements before PPC.

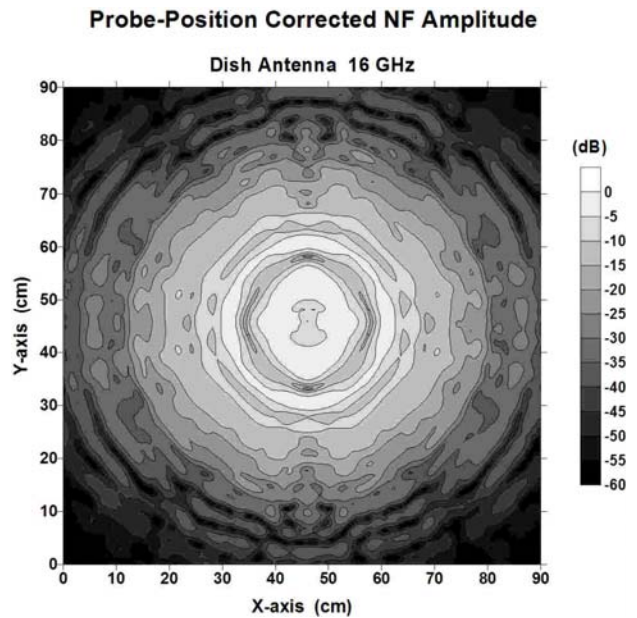


Figure 4. Near-field amplitude for 16 GHz measurements after PPC.

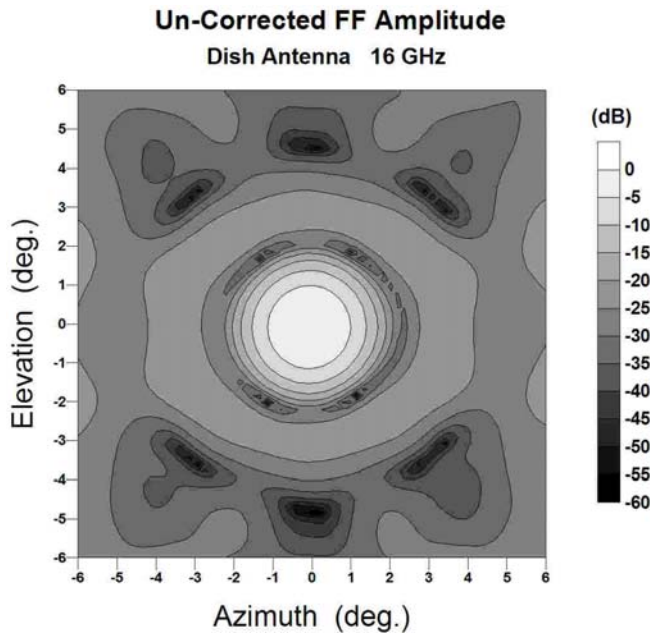


Figure 5. Coupled far-field amplitude for 16 GHz measurements before PPC.

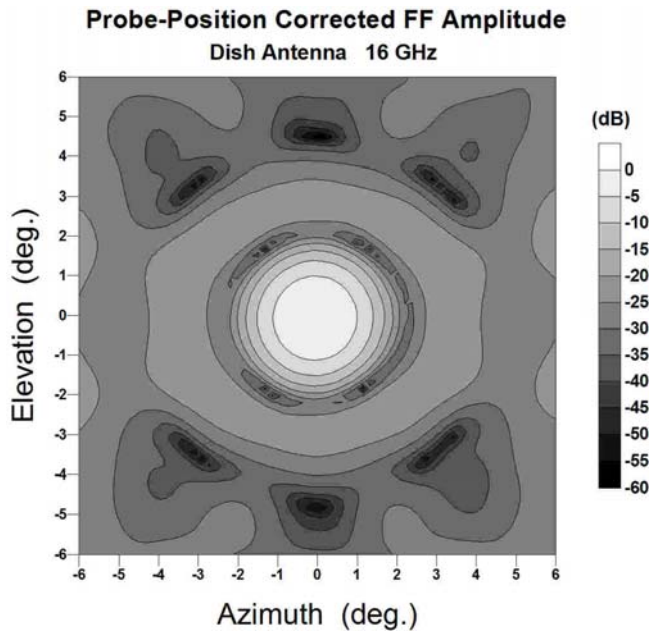


Figure 6. Coupled far-field amplitude for 16 GHz measurements after PPC.

A dish antenna and probe in the WR-22 band were used for the 35 GHz measurements. The z-position errors in the plane used in the 35 GHz measurements were as large as ± 0.01 cm (see Figure 7). According to Table 1 this is about 17% more than recommended.

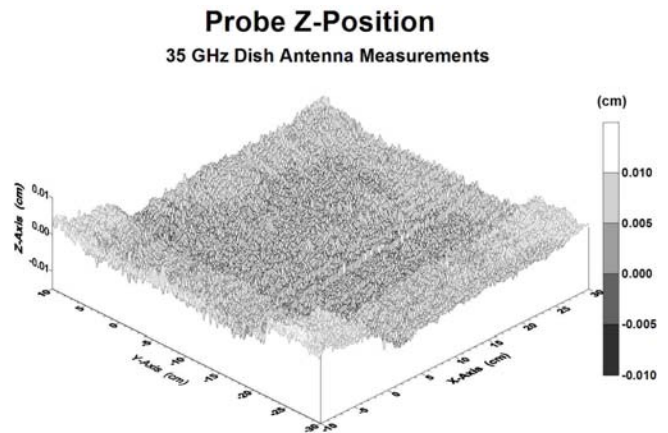


Figure 7. Probe z-position errors for 35 GHz PNF measurements.

In this case, the PPC has a more significant effect on the near-field amplitude. Figures 8 and 9 (before and after PPC) show that the PPC has made the near-field amplitude more symmetrical.

Figures 10 and 11 (the coupled far field amplitude of the measurements before and after PPC), show a similar effect for the far-field amplitude.

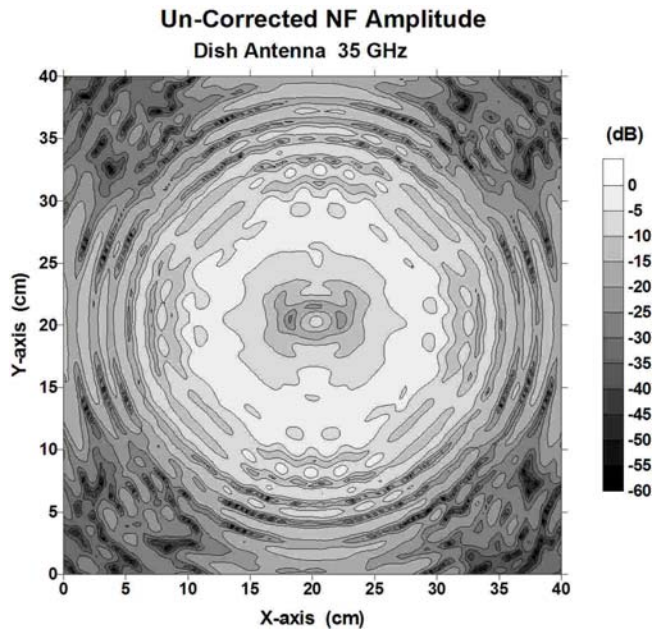


Figure 8. Near-field amplitude data for 35 GHz measurements before PPC.

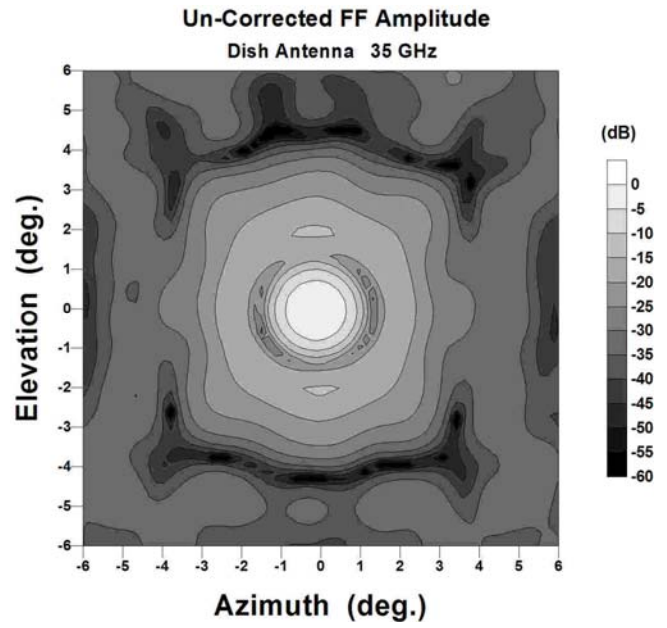


Figure 10. Coupled far-field amplitude for 35 GHz measurements before PPC.

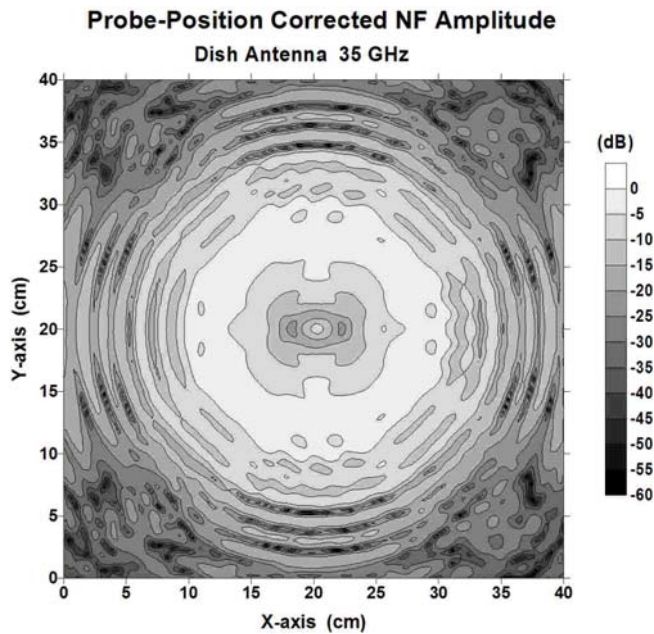


Figure 9. Near-field amplitude data for 35 GHz measurements after PPC.

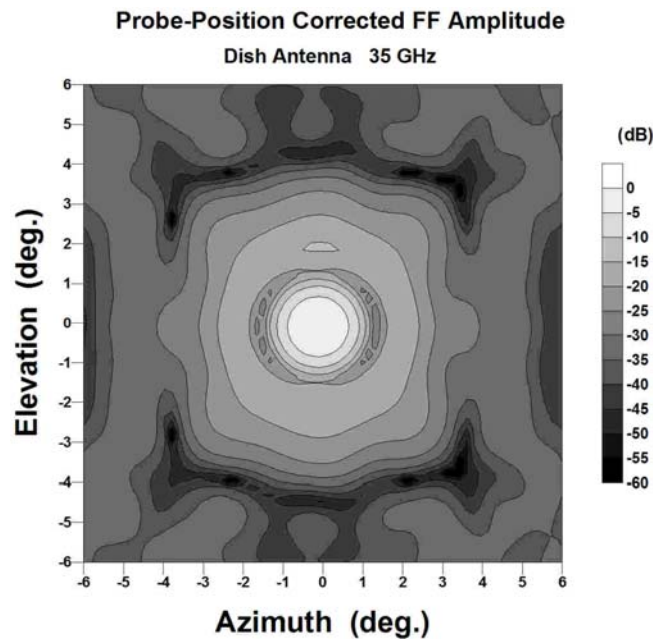


Figure 11. Coupled far-field amplitude for 35 GHz measurements after PPC.

A standard gain horn and probe in the WR-10 band were used for the 94 GHz measurements. The z-position errors, in the plane used in the 94 GHz measurements, were as large as ± 0.005 cm (see Figure 12). According to Table 1 this is about 56% more than recommended.

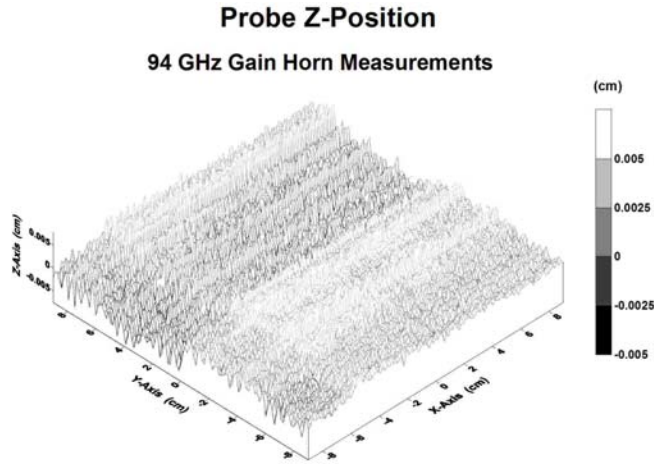


Figure 12. Probe z-position errors for 35 GHz PNF measurements.

Even though the probe position error was quite large with respect to the guidelines listed in Table 1, there was a minimal effect on the 94 GHz measurement. Figures 13 and 14, the coupled far field amplitude of the measurements (before and after PPC) show that the side-lobe levels in the principal planes were reduced.

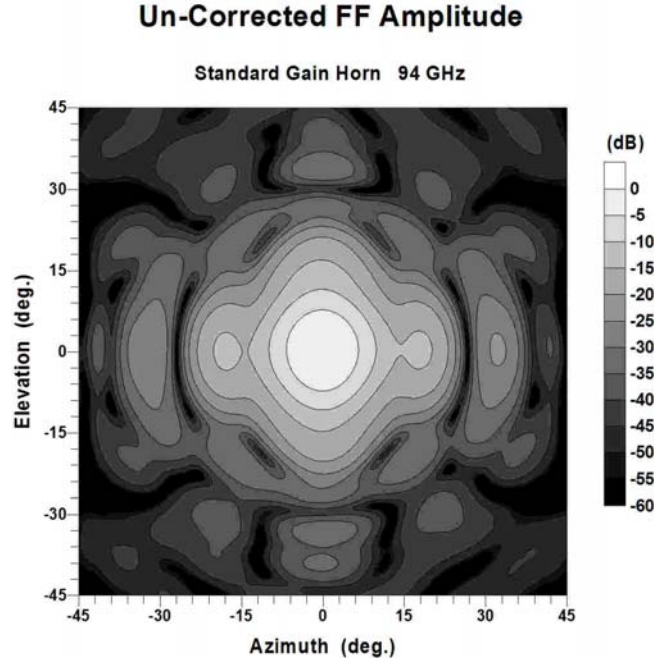


Figure 13. Coupled far-field amplitude for 94 GHz measurements before PPC.

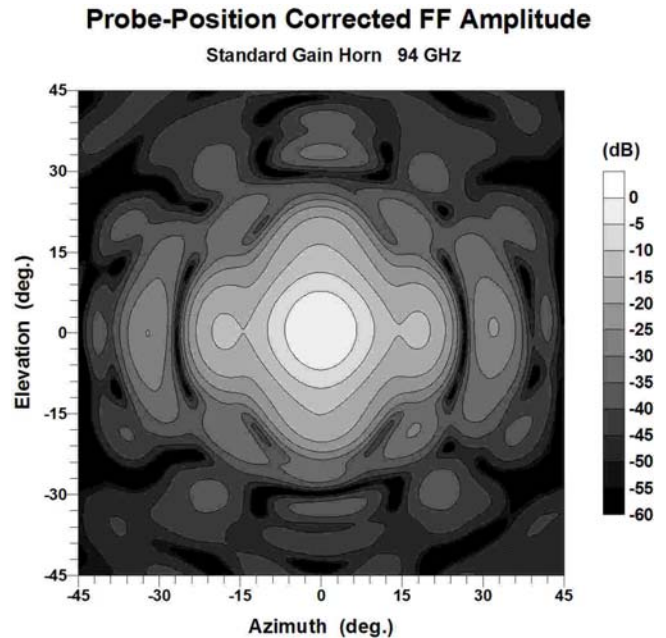


Figure 14. Coupled far-field amplitude for 94 GHz measurements after PPC.

The relative gain was also calculated for the 16, 35 and 94 GHz PNF measurements both before and after PPC. The PPC had a greater effect on the 94 GHz measurements than at 16 and 35 GHz. Table 2 lists these relative gain values.

Table 2. Relative Gain Results

16 GHz Measurements

- Uncorrected 34.94 dB ± 0.20 dB
- Probe-Position Corrected 34.96 dB ± 0.20 dB

35 GHz Measurements

- Uncorrected 41.37 dB ± 0.25 dB
- Probe-Position Corrected 41.39 dB ± 0.25 dB

94 GHz Measurements

- Uncorrected 24.92 dB ± 0.35 dB*
- Probe-Position Corrected 25.01 dB ± 0.35 dB*

**This is a best estimate because a thorough uncertainty analysis has yet to be performed at 94 GHz.*

4.0 Conclusions

This paper has shown the results of implementing a laser tracker system and using PPC on PNF measurements. We can perform measurements at frequencies above the normal limits of the PNF scanner based on mechanical positioning accuracies of the probe. From these results we can also see that our scanner yields good results at frequencies 94 GHz.

5.0 Future Work

We plan to test the robustness of the PPC algorithms by introducing gross errors in the probe's x-, y-, and z-position. Currently we are performing measurements at 110 GHz; since the scanner position accuracy is very good in the x- and y-axes we are over-sampling the data by using a spacing of $\lambda/4$. We can introduce errors in the x- and y-axes by taking points at random within $\pm \lambda/2$ of the desired measurement point. These measurements were performed on five different planes: reference plane (S_0), $S_0 + \lambda/8$, $S_0 + \lambda/4$, $S_0 + \lambda/2$, and $S_0 + \lambda$; the probe's z-position can be taken randomly from each of these scans and used in the PPC.

6.0 References

[1] J.R. Guerrieri, K. MacReynolds, M.H. Francis, R.C. Wittmann, and D.T. Tamura, **“Practical Implementation of Probe-Position Correction in Planar Near-field Measurements,”** *Proc. Ant. Meas. Assoc.*, pp 356-359, October 2004.

[2] R.C. Wittmann, B.K. Alpert, and M.H. Francis, **“Planar Near-Field Antenna Measurements Using Nonideal Measurement Locations,”** *Proc. Ant. Meas. Assoc.*, pp 74-79, October 1996.

[3] R. C. Wittmann, B. K. Alpert, and M. H. Francis, **“Near-field Antenna Measurements Using Nonideal Measurement Locations,”** *IEEE Trans. Antennas Propagat.*, vol. AP-46, pp. 43- 48, May 1988.